Article ID: 1000 - 8152(2005)01 - 0035 - 08

Pose and motion estimation from monocular vision based on IEKF, DD1 and DD2 filters

WU Xue-dong[1,2], WANG Yao-nan[1], LI Can-fei[1]

(1. College of Electrical and Information Engineering, Hunan University, Changsha Hunan 410082, China;
2. Electronic and Electrical Engineering Department, Fujian University of Technology, Fuzhou Fujian 351004, China)

Abstract: A solution to relative pose and motion estimation between two reference coordinates that used two-dimensional (2D) intensity images from a single camera was desirable for real-time applications. The difficulty in performing this measurement was that the process of projecting three-dimensional (3D) object features to 2D images was a nonlinear transformation. The system of pose and motion estimation which is based on the monocular vision was defined as a nonlinear stochastic model. The system used the iterated extended Kalman filter (IEKF), the first-order Stirling's interpolation filter (DD1) and the second-order Stirling's interpolation filter (DD2) respectively as nonlinear state estimators to estimate pose and motion. The method has been implemented with simulated data based on three kinds of different estimator respectively to show the relative advantages of each kind estimator, and the simulation result has shown that the performance of DD1 and DD2 is superior to IEKF.

Key words: line features; dual quaternion; monocular vision; iterated extended Kalman filter (IEKF); the first-order Stirling's interpolation filter (DD1); the second-order Stirling's interpolation filter (DD2); pose estimation; motion estimation

CLC number: TP391 **Document code**: A

单目视觉中基于 IEKF, DD1 及 DD2 滤波器的位姿和运动估计

伍雪冬[1,2], 王耀南[1], 李灿飞[1]

(1. 湖南大学 电气与信息工程学院, 湖南 长沙 410082; 2. 福建工程学院, 电子与电气工程系, 福建 福州 350014)

摘要: 用单摄像机所获取的二维(2D)图像来估计两坐标之间的相对位姿和运动在实际应用中是可取的, 其难点是从物体的三维(3D)特征投影到 2D 图像特征的过程是一个非线性变换, 把基于单目视觉的位姿和运动估计系统定义为一个非线性随机模型, 分别以迭代扩展卡尔曼滤波器(IEKF)、一阶斯梯林插值滤波器(DD1)和二阶斯梯林插值滤波器(DD2)作非线性状态估计器来估计位姿和运动. 为了验证每种估计器的相对优点, 用文中所提方法对每种估计器都作了仿真实验, 实验结果表明 DD1 和 DD2 滤波器的特性要比 IEKF 好.

关键词: 线特征; 八元数; 单目视觉; 迭代扩展卡尔曼滤波器(IEKF); 一阶斯梯林插值滤波器(DD1); 二阶斯梯林插值滤波器(DD2); 位姿估计; 运动估计

1 Introduction

The estimation of relative 3D position and orientation as well as relative motion between two reference frames is an important problem in robotic guidance, manipulation, assembly and in other areas such as photogrammetry, tracking, object recognition, and camera calibration[1~6]. Most measurement techniques for pose estimation are image-based and can be classified into two major categories. These categories are point-based and model-based methods using higher-order geometric primitives. Each type involves acquiring an image and processing that image to arrive at a value for the pose. Methods of point-based were the first to be studied and, as a result, have been more extensively developed than model-based method[7,8]. Line features are present in many cases to a great extent and less sensitive to noise than point features[9]. They may be more visible than points under a wider range of lighting and environmental conditions. Also, straightforward techniques such as the Hough transformation and line fitting to edges are available to extract the lines from the images[10].

To describe the relative translation and rotation between two coordinates, the usual way is by means of homogeneous transformation matrix[1~8]. Chen[11], who introduced the screw theory in the hand-eye calibration, is the first simultaneous consideration of rotation and translation in a geometric way. Daniilidis[12] uses dual quaternions that provide a means to represent both rotation and translation in a unified notation for hand-eye calibration.

When it comes to state estimation for nonlinear systems,

Received date: 2003 - 04 - 07; Revised date: 2003 - 11 - 28.

Foundation item: Supported by the Chinese National Natural Science Foundation (60375001); Hunan Provincial Natural Science Foundation of China (03JJY3107).

a series of estimators have been proposed over time, which for the most part are nonlinear extensions of the celebrated Kalman filter (KF). Up to now the extended Kalman filter (EKF) has unquestionably been the dominating state estimation technique[13,14]. The EKF is based on first-order Taylor approximation of state transition and observation equations about the state trajectory. The Taylor linearization provides an insufficiently accurate representation in many cases. Nørgaard[15] proposed a new set of estimators, namely, DD1 and DD2, which are based on polynomial approximations of the nonlinear transformations obtained with a particular multidimensional extension of Stirling's interpolation formula. The DD1 filter is based on first-order approximations and the DD2 filter is based on second-order approximations (The selection of interval length, d, was discussed in Nørgaard[16]). Conceptually, the principle underlying the DD1 and DD2 filters resembles that of the EKF and its higher-order relatives, the main difference is that matrices of divided difference replace matrix products of Jacobians and Cholesky factors of covariance matrices[17]. Moreover, in contrast to Taylor's formula no derivatives are needed in the interpolation formula, only function evaluations.

The problem proposed in this paper is to locate an object and measure its relative motion in three dimensions given a sequence of 2D images of the object whose position and orientation are known relative to a base reference frame. The 3D transformation is modeled as a nonlinear stochastic system that uses the IEKF, DD1 and DD2 respectively as the estimator, and the 3D transformation uses a screw representation based on dual quaternions. Previous solutions have used point-based image features in estimating the pose and motion. This paper uses image line features instead as measurement inputs for the estimation.

The paper is organized as follows: section 2 describes dual quaternion and the dual quaternion 3-D transformation representation is given in section 3. Section 4 presents the pinhole camera model and the line feature's representation in image plane. The pose and motion estimation system model is defined in section 5, while section 6 gives the simulation examples. Finally, the conclusion is drawn in section 7.

2 Dual quaternions

2.1 Quaternions

A Quaternion is a four-component number consisting of a scalar part and three orthogonal parts. Formally, a quaternion q can be defined as

$$q = q_0 + q_1\boldsymbol{i} + q_2\boldsymbol{j} + q_3\boldsymbol{k}. \tag{1}$$

where each of the q_i is a real number, and $\boldsymbol{i}, \boldsymbol{j}$ and $\boldsymbol{k}$ are orthogonal imaginary unit vectors. The conjugate of a quaternion is $q^* = q_0 - q_i\boldsymbol{i} - q_2\boldsymbol{j} - q_3\boldsymbol{k}$, and its modulus is $|q| = \sqrt{q_0^2 + q_1^2 + q_2^2 + q_3^2}$.

Multiplication of the two quaternions p and q is defined as

$$\begin{aligned} pq = & (p_0q_0 - p_1q_1 - p_2q_2 - p_3q_3) + \\ & (p_0q_1 + p_1q_0 + p_2q_3 - p_3q_2)\boldsymbol{i} + \\ & (p_0q_2 - p_1q_3 + p_2q_0 + p_3q_1)\boldsymbol{j} + \\ & (p_0q_3 + p_1q_2 - p_2q_1 + p_3q_0)\boldsymbol{k}. \end{aligned} \tag{2}$$

Matrix forms of quaternion multiplication are given below

$$\begin{cases} pq = \begin{bmatrix} -p_0 & -p_1 & -p_2 & -p_3 \\ p_1 & p_0 & -p_3 & p_2 \\ p_2 & p_3 & p_0 & -p_1 \\ p_3 & -p_2 & p_1 & p_0 \end{bmatrix} q = m_p^+ q, \\ qp = \begin{bmatrix} p_0 & -p_1 & -p_2 & -p_3 \\ p_1 & p_0 & p_3 & -p_2 \\ p_2 & -p_3 & p_0 & p_1 \\ p_3 & p_2 & -p_1 & p_0 \end{bmatrix} q = m_p^- q. \end{cases} \tag{3}$$

We know from equation (3) that the multiplication of quaternion is not commutative.

2.2 Dual numbers

A dual number is defined as

$$d = a + \in \bar{a}, \tag{4}$$

where $a, \bar{a}$ are real numbers and $\in$ is defined as $\in^2 = 0$, a is the real part and $\bar{a}$ is the dual part, the conjugate of a dual number d is $d^* = a - \in \bar{a}$, and its modulus is $|d| = a$. Note that the modulus of a dual number can be negative.

The Taylor series expansion of a dual function about its real part has the form

$$f(a + \in \bar{a}) = f(a) + \in \bar{a}f'(a). \tag{5}$$

2.3 Dual quaternions

A dual quaternion can be defined as

$$\hat{q} = r + \in s, \tag{6}$$

where r and s are each quaternion.

The modulus and conjugate of a dual quaternions $\hat{q}$ are $|\hat{q}| = \sqrt{\hat{q}\hat{q}^*} = \sqrt{rr^* + \in (rs^* + sr^*)}$ and $\hat{q}^* = r^* - \in s^*$.

3 Representation of 3D rotation and translation by dual number quaternions

A line in space with direction $\boldsymbol{l}$ through a point $\boldsymbol{P}$ can be represented with the 6-tuple $(\boldsymbol{l}, \boldsymbol{m})$, where $\boldsymbol{m}$ is the unit normal vector and is equal to $\boldsymbol{m} = \boldsymbol{P} \times \boldsymbol{l}$. The constraints $\boldsymbol{l} \cdot \boldsymbol{m}$ and $|\boldsymbol{l}| = 1$ guarantee that the degree of freedom of an arbitrary line in space is four.

Applying a rotation RO and a translation $\boldsymbol{t}$ to a given line $(\boldsymbol{l}_b, \boldsymbol{m}_b)$ we obtain the transformed line $(\boldsymbol{l}_a, \boldsymbol{m}_a)$

$$\begin{aligned} \boldsymbol{l}_a &= RO\boldsymbol{l}_b, \\ \boldsymbol{m}_a &= \boldsymbol{P}_a \times \boldsymbol{l}_a = (RO\boldsymbol{P}_b - \boldsymbol{t}) \times RO\boldsymbol{l}_b = \\ & RO(\boldsymbol{P}_b \times \boldsymbol{l}_b) + \boldsymbol{t} \times RO\boldsymbol{l}_b = RO\boldsymbol{m}_b + \boldsymbol{t} \times RO\boldsymbol{l}_b. \end{aligned} \tag{7}$$

We change from vector to quaternion notation which means that the vector $\boldsymbol{l}$ is represented by a quaternion with zero scalar part $l = (0, \boldsymbol{l})$. The terms containing rotation can be easily written with quaternions. The difficulty with the cross-product is tackled with the identity

$$(0, \boldsymbol{t} \times \boldsymbol{q}) = \frac{1}{2}(qt^* + tq), \tag{8}$$

where t is the translation quaternion $(0, \boldsymbol{t})$ and q is the rotation quaternion $(0, \boldsymbol{q})$. Using the identity (8) we obtain

$$\begin{aligned} l_a &= ql_bq^*, \\ m_a &= qm_bq^* + \frac{1}{2}(ql_bq^*t^* + tql_bq^*). \end{aligned} \tag{9}$$

We define a new quaternion $\bar{q} = \frac{1}{2}tq$ and a dual quaternion $\hat{q} = q + \in \bar{q}$. It can be easily shown that equation (9) is equivalent to

$$l_a + \in m_a = (q + \in \bar{q})(l_b + \in m_b)(q^* + \in \bar{q}^*). \tag{10}$$

Denoting also the lines by dual quaternions $\hat{l}_a$ and $\hat{l}_b$ we obtain

$$\hat{l}_a = \hat{q}\hat{l}_b\hat{q}^*. \tag{11}$$

This formula resembles the rotation of points with quaternions. Lines can thus be transformed using a single operation in a non-Abelian ring of dual quaternions. The norm is

$$\begin{aligned} |\hat{q}|^2 &= \hat{q}\hat{q}^* = qq^* + \in (q\bar{q}^* + \bar{q}q^*) = \\ & qq^* + \in \frac{1}{2}(qq^*t^* + tqq^*) = 1, \end{aligned} \tag{12}$$

hence $\hat{q}$ is a unit quaternion. From equation (6) and (12) we obtain

$$\hat{q} = q + \in \frac{t}{2}q = (1 + \in \frac{t}{2})q. \tag{13}$$

We know from equation (13) that the unit dual quaternion $\hat{q}$ can be written as the concatenation of a pure translation unit dual quaternion and a pure rotational quaternion with dual part equal zero.

4 Pinhole camera model and the representation of lines in a plane

A pinhole camera model, which is shown in Fig. 1, is used where the lens center is the camera reference origin. The first step is to transform the object coordinates to the camera reference. Next, the x and y coordinates of the projected object onto the image plane are found. Given image coordinates $p(x, y)$ and camera coordinates $P(x_c, y_c, z_c)$, these relations are

$$x = \frac{Fx_c}{z_c}, \; y = \frac{Fy_c}{z_c}, \tag{14}$$

where F is the focal length.

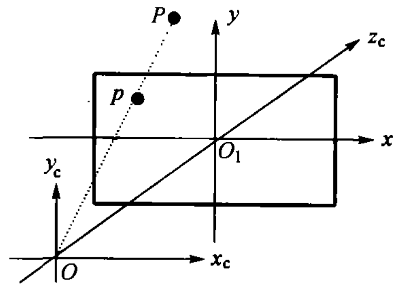

Fig. 1 Pinhole camera model

The result of the perspective projection from the 3D lines is a set of dual vector quaternion coplanar lines located in the image plane. A format is needed to compare these transformed lines with line features measured from the acquired images. The format used to represent these lines is an x, y point called the line point. A line point is defined as the intersection of the line feature with a line passing through the image origin that is perpendicular to the line feature. Fig. 2 illustrates the definition of the line point on the image plane. The line point is unique for all lines except for those lines that pass through the origin. The line point has the advantage of minimum state representation and a simple distance measure as well as being continuous for all lines.

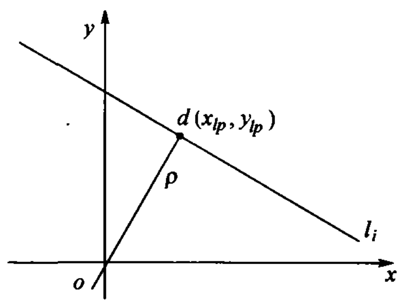

Fig. 2 Definition of line point in 2D image plane

The projected line lies in a plane defined by the 3D line and the center of projection. This plane is described by the equation

$$m_x x_c + m_y y_c + m_z z_c = 0, \tag{15}$$

that intersects the image plane at $z_c = F$. The result is an equation of the projected line in the $z_c = F$ plane,

$$m_x x_i + m_y y_i + m_Z F = 0, \tag{16}$$

where x_i and y_i are the image plane coordinates. The direction vector of the image line is

$$l_i = \left[-\frac{m_y}{\sqrt{m_x^2 + m_y^2}} \quad \frac{m_x}{\sqrt{m_x^2 + m_y^2}} \quad 0 \right]^{\mathrm{T}}. \tag{17}$$

The line point is calculated from the dual vector image line as

$$x_{lp} = l_{iy} m_{iz},\ y_{lp} = -l_{ix} m_{iz}. \tag{18}$$

In terms of the 3D dual vector components,

$$x_{lp} = F\frac{m_x m_z}{m_x^2 + m_y^2},\ y_{lp} = F\frac{m_y m_z}{m_x^2 + m_y^2}. \tag{19}$$

5 Model of pose and motion system

Consider the following general nonlinear model of a dynamic system whose states are to be estimated

$$x_{k+1} = f(x_k, v_k),\ y_k = h(x_k, w_k), \tag{20}$$

v_k and w_k are assumed i.i.d. and independent of current and past states, $v_k \sim (\bar{v}_k, Q(k))$, $w_k \sim (\bar{w}_k, R(k))$.

The state assignment estimates the transformation between the camera and the object reference frames and the first derivatives of this transformation. The assignment is based on the dual quaternion representation of the 3D transformation. Similar to the approach given by Broida[18], the state variable assignment with a known object geometry is

$$x_k = [t_x \quad t_y \quad t_z \quad q_0 \quad q_1 \quad q_2 \quad q_3 \quad v_x \quad v_y \quad v_z \quad \omega_x \quad \omega_y \quad \omega_z]^{\mathrm{T}}. \tag{21}$$

Thirteen state variables are present: t_i and v_i terms are the linear translation and linear velocity, respectively, q_i is the rotational quaternion, and ω_i is the rotational velocity in each axis. Translation, rather than the dual part of the dual quaternion, is estimated in the state vector since the dual part can readily be calculated from the translation and rotational real quaternion as given by equation (13). The first derivative is

$$\dot{\hat{q}} = \dot{q} + \epsilon\left(\frac{\dot{t}}{2} q + \frac{t}{2}\dot{q}\right). \tag{22}$$

Chou[19] gives the relation between quaternion angular velocity and the spatial angular velocity

$$\Omega = [0 \quad \omega_x \quad \omega_y \quad \omega_z]^{\mathrm{T}} = 2\dot{q}q^*. \tag{23}$$

Ω is a vector quaternion where the vector portion is the angular velocity about the axis. Solving for $\dot{q}$

$$\dot{q} = \frac{1}{2}\Omega q. \tag{24}$$

Since the quaternion has four parameters to represent rotation, and additional degree of freedom is present. As a result, normalization of the quaternion to unit magnitude is performed after each iteration.

The state transition function $f(x_k, v_k)$ extrapolates from the state at time interval k to the next state at time interval $k+1$. The linear and angular velocities are assumed constant so that $\omega_i(k+1) = \omega_i(k)$ and $v_i(k+1) = v_i(k)$.

The quaternion propagation in time is described by equation (24), the solution is when all ω_i are constant, after simplication

$$q(t_{k+1}) = [\cos(|\omega|(\tau)/2)I + \frac{2}{|\omega|}\sin(|\omega|(\tau)/2)\Omega]q(t_k) = Q_t q(t_k), \tag{25}$$

where τ is the sampling time.

The complete state transition function is

$$x_{k+1} = [t_x + \tau v_x \quad t_y + \tau v_y \quad t_z + \tau v_z \quad Q_t q(t_k) \quad v_x \quad v_y \quad v_z \quad \omega_x \quad \omega_y \quad \omega_z]^{\mathrm{T}}. \tag{26}$$

Measurement function $h(x_k, w_k)$ comprises the line point function given in equation (19). Since the dual quaternion operation transforms lines to lines, the given model features from the object are lines represented as dual vector quaternions. The measured $y_k = h(x_k, w_k)$ components are the line points of the 2D image plane lines projected from the 3D lines.

For the parameter m of measurement function $y_k = h(x_k, w_k)$, according to equation (7) and (11), expanding each line, $l + \epsilon\, m$, and solving for m gives

$$m = m_r^+ m_r^{-*} m_m + \frac{1}{2} m_t^{-*} m_r^+ m_r^{-*} l_m + \frac{1}{2} m_t^+ m_r^+ m_r^{-*} l_m = m_r^+ m_r^{-*} m_m + \frac{1}{2}(m_t^+ + m_t^{-*}) m_r^+ m_r^{-*} l_m, \tag{27}$$

where m_m is the initial normal vector and m is the normal vector after transformation. Let $RO = m_r^+ m_r^{-*}$ and $M = m_t^+ + m_t^{-*}$. RO and M can be computed from equation (3).

6 Simulation experiments

To demonstrate the performance of the three kinds of filter, a target object is simulated with individual feature points. Pairs of these points, when extracted from the image plane, are connected together to form lines. For the test, an object with four coplanar points in a rectangular pattern was defined. Fig. 3 shows the dimensions and the shape of the four points target.

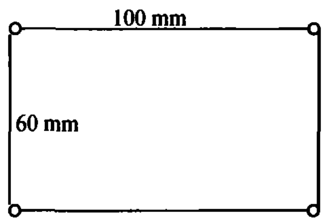

Fig. 3 Four-point coplanar target used in the simulation experiment

The object of the filter is to estimate the position, orientation, and corresponding velocities of the object with respect to the camera. The noisy image plane feature locations are used as inputs along with a priori knowledge. An ideal camera model is used in the simulation. Perspective projection is assumed for the camera with a known effective focal length. Noise of an assumed magnitude and distribution is added to the image feature locations before processing.

Initial conditions requiring specification include the initial state, x_0, and the error covariance matrix P_0. The state vector may be considered a collection of Gaussian random variables with covariance P_0. The initial state is a sampling taken from each random variable. Process noise given by the covariance matrix Q is also specified as an initial condition for the simulations, remaining constant throughout. Similarly, measurement noise given by the covariance matrix R is initially specified as a constant and the diagonal elements are 0.0004 mm.

To compare the performance of IEKF, DD1 and DD2, we took two groups assumed initial states to estimate the pose and motion. The assumed initial state and the true initial state are shown in table 1. The diagonal elements of the initial error covariance matrix P_0 and the process noise matrix Q are shown in table 2. The input noise is a Gaussian with a standard deviation of 0.02 mm. Based on this noise level, the measurement error covariance matrix has diagonal elements of 0.0004 mm^2 for each measured variable.

Table 1 Actual and assumed initial state

State	Translation (mm)			Quaternion				Linear Velocity (mm·s^{-1})			Rotational Velocity (rad·s^{-1})		
	x	y	z	q_0	q_1	q_2	q_3	x	y	z	x	y	z
True initial state	10	10	1000	1	0	0	0	−5	2	−5	−0.03	0.05	−0.2
Assumed initial state Ⅰ	0	0	990	0.998	0.01	0.01	0.01	−4.5	1.5	−4.5	−0.028	0.045	−0.15
Assumed initial state Ⅱ	0	0	900	0.9	0.1	0.1	0.01	0.01	0.01	0.01	0.01	0.01	0.01

Table 2 The diagonal elements of initial error covariance matrix and process noise matrix

State	Translation (mm)			Quaternion				Linear Velocity (mm·s^{-1})			Rotational Velocity (rad·s^{-1})		
	x	y	z	q_0	q_1	q_2	q_3	x	y	z	x	y	z
P_0	100	100	100	0.01	0.01	0.01	0.01	100	100	100	0.1	0.1	0.1
Q	10^{-5}	10^{-5}	10^{-5}	10^{-5}	10^{-5}	10^{-5}	10^{-5}	10^{-5}	10^{-5}	10^{-5}	10^{-5}	10^{-5}	10^{-5}

To ensure a fair result of the estimation result proposed in this paper, the estimates are averaged across a Monto Carlo simulation consisting of 50 runs. Each run is carried out with a different noise sample, and the simulation was run for a time of 30 seconds with a measurement interval of 0.1 second. The pose and motion estimation results of the Monto Carlo simulation with the assumed initial state Ⅰ are shown in Fig. 4 (The iterative steps is 20 for the IEKF filter), and the pose and motion estimation results of the Monto Carlo simulation with the assumed initial state Ⅱ are given in Fig. 5 (The simulation results are diverge for IEKF filter when the iterative steps varies from 1 to 50).

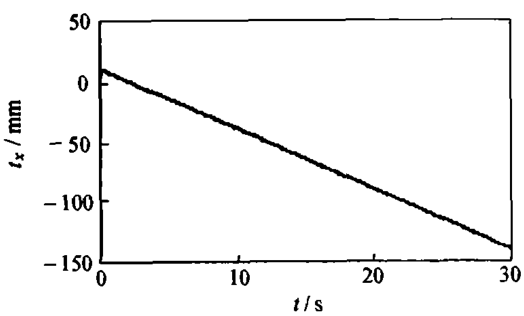

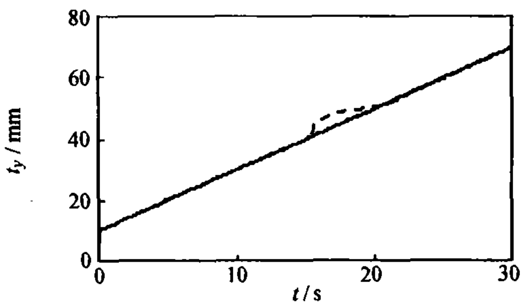

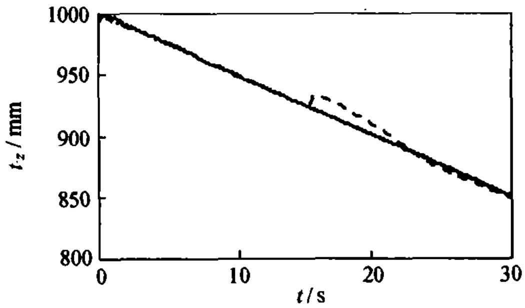

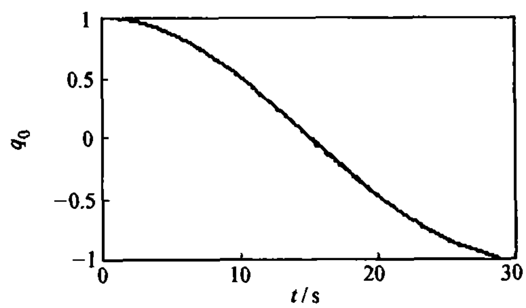

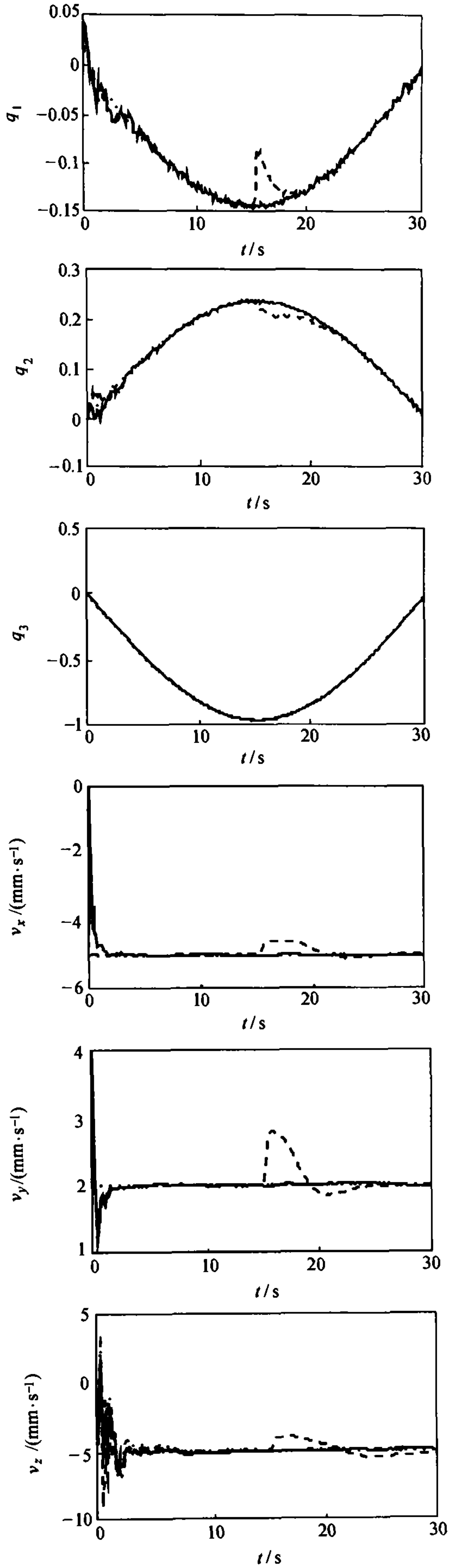

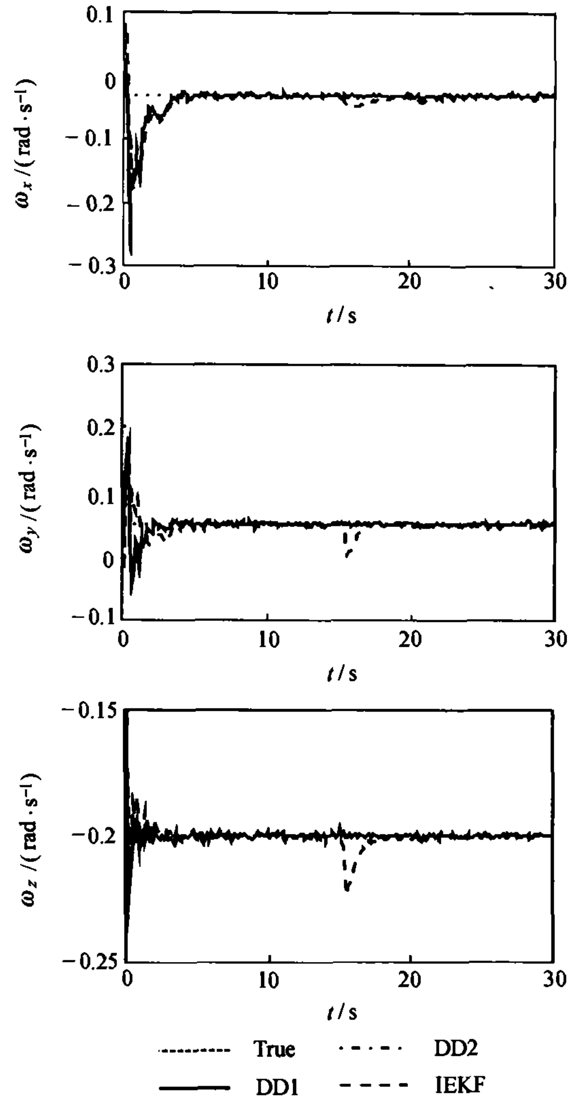

Fig. 4 Simulation results of pose and motion estimation with initial state value (0,0,990,0.998,0.01, 0.01,0.01,−4.5,1.5,−4.5,−0.028, 0.045,−0.15).(50 runs average)

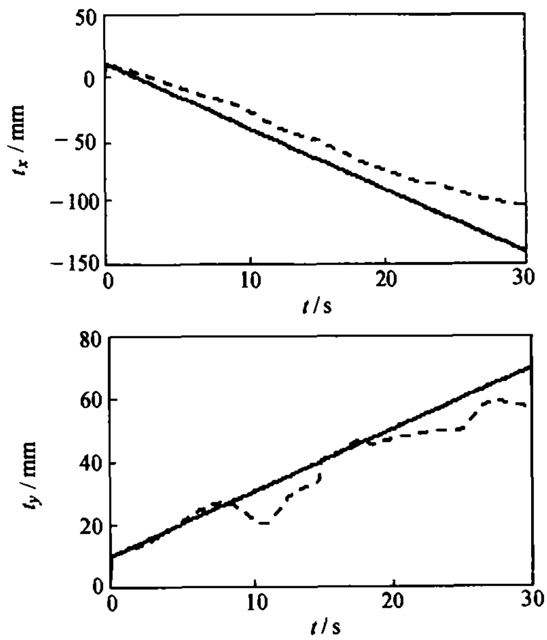

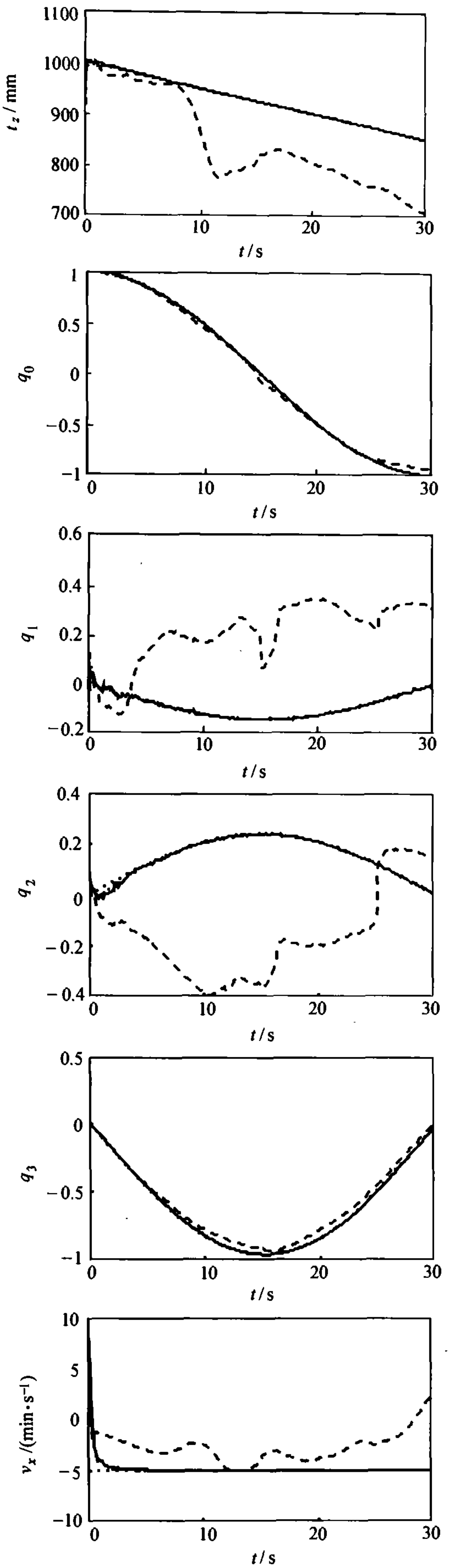

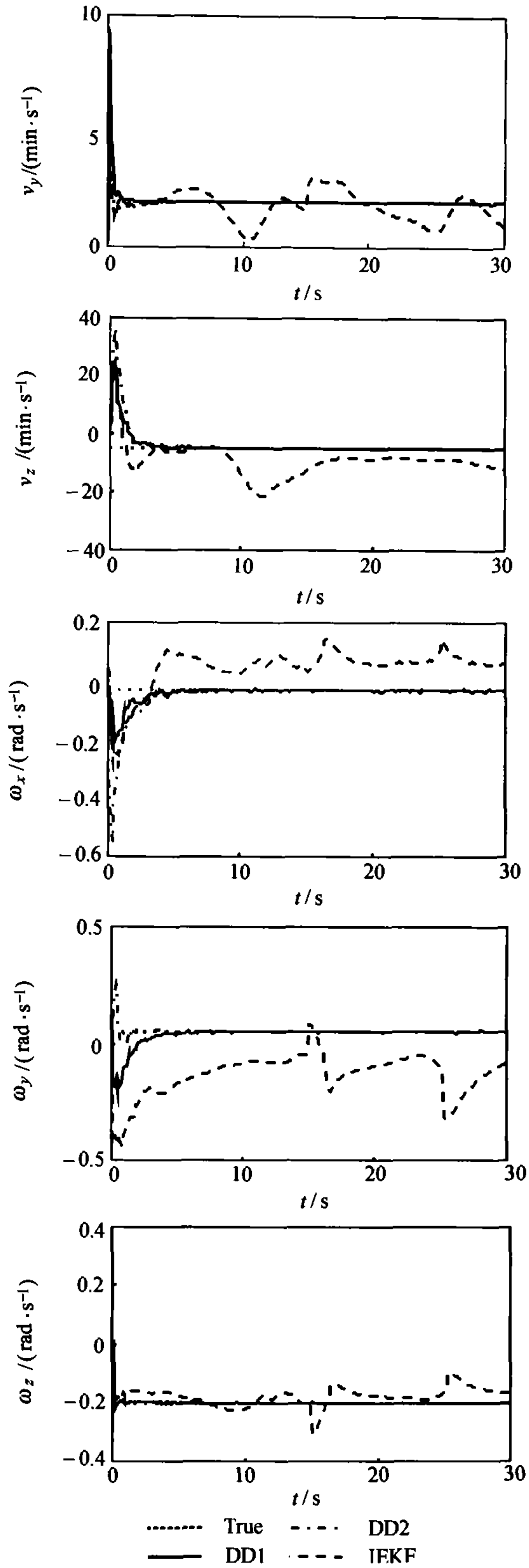

Fig. 5 Simulation results of pose and motion estimation with initial state value (0,0,990,0.9,0.1,0.1,0.01, 0.01,0.01,0.01,0.01,0.01,0.01). (50 runs average).

7 Conclusion

Three kinds of pose and motion estimation methods have been developed. These methods use an imaging technique with a single area-based camera along with a reference object to calculate estimates for relative six-degree of freedom position and orientation as well as the associated velocity estimates. The system model for these methods are based on line features, a dual quaternion parameterization for the 3-D transformation, using IEKF, DD1 and DD2 as estimator respectively. Conceptually, the principle underlying the DD1 and DD2 filters resembles that of the EKF and its higher-order relatives. The implementation is, however, quite different. In contrast to Taylor's formula no derivatives are needed in the interpolation formula, only function evaluations. From the simulation results of two groups assumed initial states, we conclude that when the assumed initial state is near to the true initial state, the IEKF, DD1 and DD2 filters all can converge to the true state, but the performance of IEKF is slightly worse than DD1 and DD2, however, as the assumed initial state is far from the true initial state, the IEKF filter is diverge from the true state, while the DD1 and DD2 filters have good convergence.

References:

[1] ZHANG Z. Motion of an uncalibrated stereo rig: self-calibration and metric reconstruction [J]. *IEEE Trans on Robotics and Automation*, 1996, 12(1): 103 - 113.

[2] ZHUANG H. Hand-eye calibration for electronic assembly robots [J]. *IEEE Trans on Robotics and Automation*, 1998, 14(4): 612 - 616.

[3] MA S. A self-calibration technique for active vision systems [J]. *IEEE Trans on Robotics and Automation*, 1996, 12(1): 114 - 120.

[4] SHIU Y. Calibration of wrist-mounted robotic sensors by solving homogeneous transform equations of the form $AX = XB$ [J]. *IEEE Trans on Robotics and Automation*, 1989, 5(1): 16 - 29.

[5] DORNAIKA F. Simultaneous robot-world and hand-eye calibration [J]. *IEEE Trans on Robotics and Automation*, 1998, 14(4): 16 - 27.

[6] LI, M. Kinematic Calibration of an active head-eye system [J]. *IEEE Trans on Robotics and Automation*, 1998, 14(1): 153 - 157.

[7] WILSON J. Relative end-effector control using Cartesian position based visual servoing [J]. *IEEE Trans on Robotics and Automation*, 1996, 12(5): 684 - 696.

[8] WANG J. 3d relative position and orientation estimation using Kalman filter for robot control [C]// *Proc of IEEE Trans on Robotics and Automation*. Nice, France: IEEE Press, 1992, 5: 2638 - 2643.

[9] LIAO X. *Computer vision system for an autonomous mobile robot* [EB/OL]. Cincinnati, Ohio: The Center for Robotics Research, University of Cincinnati, (2000-4) [2001-11]. http://www.robotics.uc.edu/papers/Spie2000.htm.

[10] TALLURI R. Mobile robot self-location using model-image feature correspondence [J]. *IEEE Trans on Robotics and Automation*, 1996, 12(1): 63 - 77.

[11] CHEN H. A Screw motion approach to uniqueness analysis of head-eye geometry [C]// *IEEE Conf on Computer Vision and Pattern Recognition*. Mau, KI, USA: IEEE Press, 1991(1): 145 - 151.

[12] DANIILIDIS K. Hand-eye calibration using dual quaternions [J]. *Int J of Robotics Research*, 1999, 18(3): 286 - 298.

[13] LIPPIELLO V. Objects motion estimation via BSP tree modeling and Kalman filtering of stereo images [C]// *IEEE Conf on Robotics and Automation*. Washington, DC: IEEE Press, 2002, 3: 2968 - 2973.

[14] LIPPIELLO V. Position and orientation estimation based on Kalman Filtering of stereo images [C]// *IEEE Conf on Control Applications*. México City, México: IEEE Press, 2001, 1: 702 - 707.

[15] NØRGAARD M. New developments in state estimation for nonlinear systems [J]. *Automatica*, 2000, 36(8): 1627 - 1638.

[16] NØRGAARD M. *Advances in derivative-free state estimation for nonlinear systems, IMM-REP*-1998-15 [R]. Denmark: Technical University of Denmark, 1998.

[17] SCHEI T. A finite-difference method for linearization in nonlinear estimation algorithms [J]. *Automatica*, 1997, 33(11): 2051 - 2058.

[18] BROIDA J. Recursive 3-d motion estimation from a monocular image sequence [J]. *IEEE Trans on Aerospace and Electronic Systems*, 1990, 26(4): 639 - 656.

[19] CHOU K. Quaternion kinematic and dynamic differential equations [J]. *IEEE Trans on Robotics and Automation*, 1992, 8(2): 53 - 64.

作者简介:

伍雪冬 (1975—),男,博士,研究兴趣为计算机视觉,图像处理,机器人和智能控制,E-mail: woolcn@163.com;

王耀南 (1957—),男,博士,教授,博士生导师,主要从事智能控制理论与应用,计算机视觉,图像识别和机器人等研究工作;

李灿飞 (1977—),女,博士生,研究领域为图像融合,计算机视觉.